Expansion and radiative cooling of the laser induced plasma

Sy-Bor Wen, Xianglei Mao, Chunyi Liu, Ralph Greif and Richard Russo

Lawrence Berkeley National Laboratory, Berkeley, CA 94720

E-mail: rerusso@lbl.gov

Abstract. To study the expansion and cooling process of the laser induced plasma generated by nanosecond pulsed laser ablation, experiments have been conducted which measure the position of the external shockwaves and the temperature of the vapor plumes. The positions of external shockwaves were determined by a femtosecond laser time-resolved imaging system. Vapor plume temperature was determined from spectroscopic measurements of the plasma emission lines. A model which considers the mass, momentum, and energy conservation of the region affected by the laser energy was developed. It shows good agreement to the experimental data.

1. Introduction

Pulsed laser ablation is the technique that involves applying a large amount of laser energy over a short duration to a sample surface. Violent melting and evaporation of the sample material results in a fast expanding high temperature vaporized plume above the sample surface. The initial temperature of this vapor plume is generally greater than 10,000K and almost all of the mass is ionized. This highly ionized vapor plume (or plasma) emits spectral radiation which can be utilized to determine the composition of the sample, as well as provide fundamental information on the ablation process.

To understand spectral emission and condensation processes in the vapor plume, the size, temperature, and pressure of the vapor plume must be determined in advance. In this paper, we present a theoretical analysis which can be used to determine these values during the expansion and cooling processes. The simulation data for the position of the shockwave (Fig. 1a) and temperature of the vapor plume (Fig. 2) are compared to experimental measurements for verifying the accuracy of the model. The presence of a shockwave within the vapor plume during simulation (Fig. 1a) is also correlated to the possible mechanisms of particle generation (Fig. 3) after the laser ablation process.

2. Experiment setup

A Nd:YAG laser with a 4-ns pulse and a Ti: sapphire laser with a 100-fs pulse were used in the experiments. For measuring shadowgraph images, the nanosecond pulsed laser at 266nm with E=0.25mJ was used as the ablation laser; the femtosecond pulsed laser was used as the probe beam. The femtosecond laser formed a probe beam at 400 nm that was perpendicular to the ablation laser beam. The probe beam was directed to a CCD camera after passing through a narrowband 400 nm filter. The time delay between the fs probe and ns ablation beams was controlled by using a delay generator. The actual delay time was measured using photodiodes in the optical paths. The position of the external shockwave can be determined from these shadowgraph images.

The nanosecond pulsed laser operating at 1064 nm with a 4-ns pulse-duration and E=20mJ was used as the ablation source for measuring the temperature of the vapor plume. The laser beam was focused on the copper sample to a spot diameter of 174 μm. A lens was used to image the laser-

induced plasma onto the entrance slit of a spectrometer. The spectral emission was detected by using an Intensified Charge-Coupled Device (ICCD) system with 1024×1024 pixels. The dark current background of the ICCD detector was subtracted from the measured spectroscopic data for each measurement. A delay generator was used to synchronize the delay time between the laser and the ICCD. Gating the ICCD and changing the delay time enabled the images and spectra to be temporally resolved. The gate width was set at ten percent of the delay time. A photodiode and a digitizing oscilloscope were used to calibrate the time delay.

Under optically thin conditions for the two lines using for evaluating the temperature of the vapor plume, the temperature can be related to the line intensities according to the following relation

$$\frac{\varepsilon_1}{\varepsilon_2} = \frac{\lambda_2}{\lambda_1}\frac{A_{ul,1}}{A_{ul,2}}\exp(-\frac{E_{u,1}-E_{u,2}}{kT}) \tag{1}$$

The spectral emission lines for Cu(I) at 511.19 and 529.81 nm were used to determine the plasma temperature. These intensities remain sufficiently large to permit detection up to tens of microseconds after the laser pulse. All experiments were down in the air with one atmospherical pressure.

3. Theoretical analysis

The analysis addresses the expansion and cooling of the laser induced vapor plume into background air from a few picoseconds to about a hundred microseconds after the laser pulse. Mass, momentum, and energy conservation with radiation as the only heat transport, Saha's equation, and equations of state are used as the governing equations. Density, pressure, and temperature, along with the positions of shockwaves and the contact surface between the vapor plume and background gas are determined during the simulation. Jump conditions of density, pressure, temperature, and velocity behind a shockwave are used as boundary conditions for regions divided by shockwaves. At the contact surface, pressure and velocity are required to be the same. The radiative heat loss in the energy conservation equation is composed of line, free-free, and free-bound emission. The integral method was used in the analysis; the integral form of mass, momentum, and energy conservation relations for each region for a spherical symmetric expansion structure are given as follows.

$$\frac{d}{dt}\left(\int_{R_{l,i}}^{R_{u,i}} 2\pi\rho_i r^2 dr\right) = 2\pi R_{l,i}{}^2\rho_{i-1}V_{i-1} - 2\pi R_{l,i}{}^2\rho_{i+1}V_{i+1} \tag{2}$$

$$\frac{d}{dt}\left(\int_{R_l}^{R_u} \rho_i V_i \pi r^2 dr\right) = \pi R_{i-1}{}^2 p_{i-1} - \pi R_{i+1}{}^2 p_{i+1} + \int_{R_l}^{R_u} p_i 2\pi r dr \tag{3}$$

$$\frac{d}{dt}\left[\int_{R_l}^{R_u}\left(\frac{1}{2}\rho_i V_i^2 + \frac{p_i}{\gamma_i-1}\right)2\pi r^2 dr\right] = -2\pi\left[R_u{}^2 p_{i+1} + \frac{\gamma_{i+1}p_{i+1}}{\gamma_{i+1}-1}\left(\dot{R}_{i+1}-V_{i+1}\right)R_u{}^2 + R_l{}^2 p_{i-1} - \frac{\gamma_{i-1}p_{i-1}}{\gamma_{i-1}-1}\left(\dot{R}_{i-1}-V_{i-1}\right)R_l{}^2\right] - Q_{rad} \tag{4}$$

where ρ is the density, p is the pressure, R_i is the lower boundary radius, R_u is the upper boundary radius, γ is the specific heat ratio, and Q_{rad} is the heat loss due to thermal radiation in the region considered. The subscript i refers to the quantity in the region i, and the subscripts i-1 and i+1 refer to quantities of regions just before and after region i.

Two conditions have been studied using the model. The first case focuses on the time interval between zero to ~1 μs after the laser pulse. The second case focuses on the time interval from a few μs to about one hundred μs after the laser pulse. In the first case, from zero to ~1 μs, only continuum emission is strong [1], the energy loss by continuum emission is small compared to the total energy of the vapor plume before 1 μs. Thus, vapor plume can be considered as undergoing an adiabatic expansion process. As a result, the energy loss due to radiative heat transfer can be omitted in this time interval. For the second case (at longer times), since shockwaves decay to sound waves, the vapor plume can be considered as undergoing a radiative cooling process with a pressure equal to the pressure of the background gas. Hence, the momentum equation is not necessary in the simulation for this time interval. The propagation of shockwaves in the first case and the temperature variation of the vapor plume in the second case are plotted separately in Fig.1 and 3

4. Results and Discussion

4.1 From zero to ~10's of ns after the laser pulse (Strong Expansion)

With most of the laser energy is converted to the kinetic energy of the vapor plume, the expansion speed of the vapor plume is close to the free expansion speed (Fig. 1b), $v_{vapor} = \sqrt{16E_v / 3M_v}$, where E_v is the laser energy in the vapor plume and M_v is the mass of the vapor plume. By measuring the early expansion speed of the vapor plume from shadowgraph images, the E_v / M_v ratio within the vapor plume can be determined by the above relation.

4.2 From ~10's of ns to ~100's of ns after the laser pulse (Slow Expansion)

The propagation of the external shockwave follows the relation, $r = C_1 (E / \rho_1)^{1/5} t^{2/5}$, according to the approximate treatment of a strong explosion proposed by Chernyi [2] (Fig. 1c). Even though this relation is similar to Sedov's law (differing only in the value of the first constant), the density, pressure, and temperature distribution predicted by Sedov's law from the center to the edge of the external shockwave cannot be used to describe these properties within the vapor plume due to the presence of an additional vapor plume inside the external shockwave region.

The internal shockwave starts to move back toward the sample surface (Fig. 1a). When the internal shockwave strikes the surface, large pressure gradients are produced, which can result in liquid ejection. Pressure gradient along the boundary of the liquid pool can push melted material outward forming a cone shaped liquid sheet (Fig. 3a for copper, Kelvin-Helmholtz instability [3]); Pressure gradient normal to a boundary of the liquid pool can cause the melted material to be ejected as a string of round liquid droplets (Fig. 3b for silicon, Richtmyer-Meshkov instability [4]).

4.3 From ~100's of ns to ~10's of μs after the end of laser pulse (Radiative cooling)

Both the internal and external shockwaves decay to sound waves ~1 ns after the laser pulse (Fig. 1 a); the temperature within the vapor plume can be considered to be uniform. The decrease of the vapor plume temperature is the same as that described in the second case of simulation, which does not consider gas dynamic effects and only includes radiative heat transfer. The temperature predicted from this case is shown in figure 2. The simulation is in excellent agreement with the experiment data.

5. Conclusions

A detailed analysis was made of the vapor plume expansion and cooling process for high energy laser ablation by using a gas dynamic model with radiative heat transfer. The predicted external shockwave position from zero to ~1 μs and the changing rate of the vapor plume temperature from a few μs to tens of μs showed excellent agreement with experimental data. The shadowgraph images show the possibility of fluid instabilities when the internal shockwave strikes the molten sample surface, which could be one of the major mechanisms of mass removal and particle generation after laser ablation.

References

[1] Ho J R J, Grigoropoulos C P and Humphery J A C 1996 *J. Appl. Phys.* **79** 7205-15
[2] Zel'dovich Y B and Raizer Y P 1966 ***Physics of Shock Waves and High-Temperature Hydrodynamic Phenomena*** (New York: Academic Press)
[3] Drazin P G and Reid W H 1981 ***Hydrodynamic stability*** (Cambridge: Cambridge University Press)
[4] RICHARD L H, GUY D, BRUCE F, MICHAEL L G, JOHN W G, MARILYN S, DAVID H S, ALEXANDER L V, ROBERT P W AND QIANG Z 1999 *J. Fluid Mech.* **389** 55-79
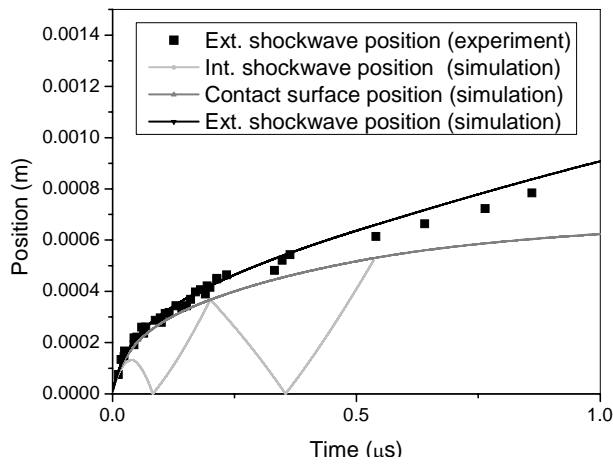
(a)
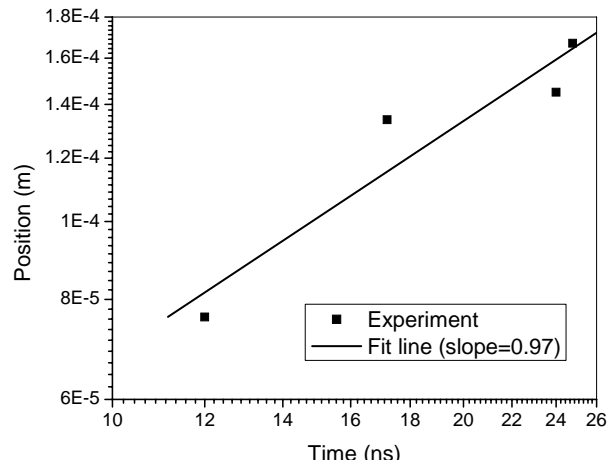
(b)
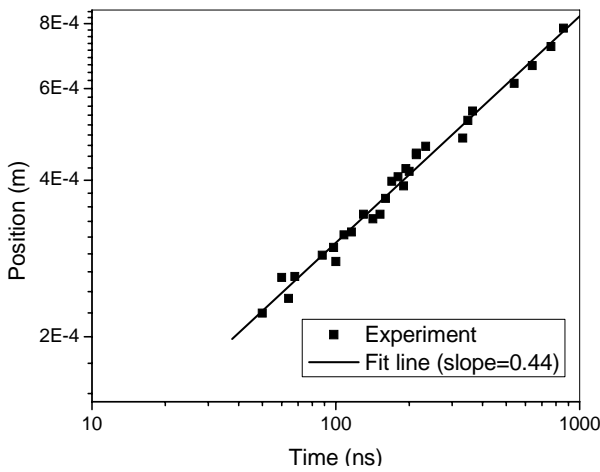
(c)

Figure 1. (a) Comparison between the simulated position of the external shockwave with the experiment for laser ablation on a copper surface with laser energy E=0.25mJ (theoretical fitting energy E=0.2mJ) and M~1.5×10^{11}kg (b) The position of the external shockwave increase as $t^{0.97}$ shortly after the laser pulse, which is close to free expansion (c) The position of the external shockwave increases as $t^{0.44}$ from ~10's ns to ~100's ns after the laser pulse, which is close to a blast wave.
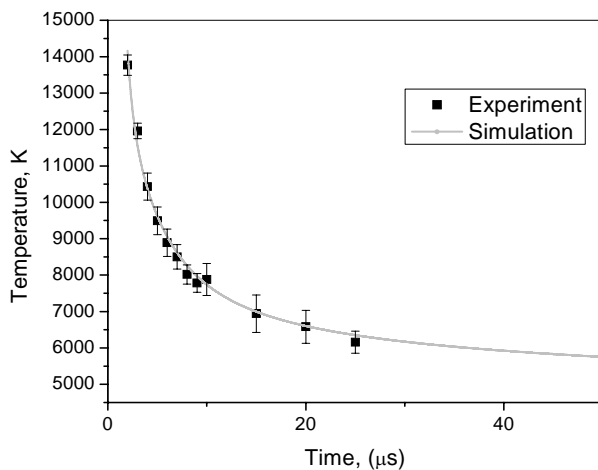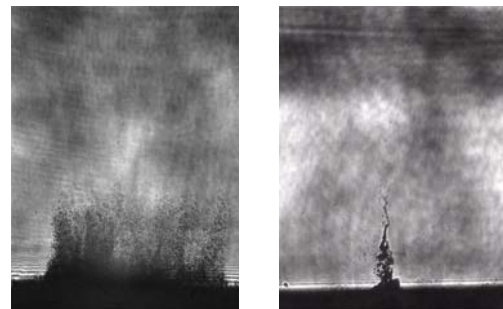

Figure 2. Comparison between the experimental measurement of the temperature variation of the vapor plume and the simulation result when E=20mJ.

(a) Copper   (b) Silicon

Figure 3. Liquid metal ejection from the surface for (a) Copper sample at 216 ns after the laser pulse (b) Silicon sample at 336 ns after the end of the laser pulse